

# On local and non-local energy transfers in Hall magnetohydrodynamic turbulence

Arijit Halder<sup>1</sup>, Supratik Banerjee<sup>1†</sup>, Pablo D. Mininni,<sup>2</sup> and Manohar K. Sharma<sup>3</sup>

<sup>1</sup>Department of Physics, Indian Institute of Technology, Kanpur 208016, India

<sup>2</sup>Universidadde Buenos Aires, Facultad de Ciencias Exactas y Naturales, Departamento de Física, and CONICET - Universidad de BuenosAires, Instituto de Física Interdisciplinaria y Aplicada (INFINA), Ciudad Universitaria, 1428 Buenos Aires, Argentina

<sup>3</sup>Department of Applied Physics and Science Education Eindhoven University of Technology, Eindhoven 5612AP, The Netherlands

(Received xx; revised xx; accepted xx)

A systematic study of inertial energy cascade in three-dimensional Hall magnetohydrodynamic turbulence is conducted to probe into the locality of energy conserving triads and the subsequent transfers. Using direct numerical simulations, we calculate the shell-to-shell energy transfer rates corresponding to **b-to-b** (magnetic to magnetic) and **j-to-b** (current to magnetic) channels due to the Hall term (Halder *et al.* (2023); Banerjee & Halder (2024)), and convincingly show that both channels comprise of a combination of local and non-local energy transfers. A local inverse transfer is consistently observed at all scales of the **b-to-b** channel whereas for the **j-to-b** channel, the transfer due to local interactions shows a transition from a weak inverse to a strong direct cascade across the Hall scale. Calculating mediator-specific transfer rates, we also conclude that a considerable amount of local energy transfer is mediated by the non-local triads, especially at small-scales of **j-to-b** transfer. Assuming power-laws for the modal fields, we offer heuristic arguments for some of our observed results. The present study captures the intricate dynamics of energy transfer due to the Hall term and hence can be used to develop more insightful analytical models (shell models for example) for Hall magnetohydrodynamic cascade and to carefully segregate the local and the non-local heating in the space plasmas.

## 1. Introduction

Meticulous understanding of plasma turbulence is essential for explaining different nonlinear phenomena in space and astrophysics. At length scales superior to the ion inertial length ( $d_i$ ), plasma behavior is described by magnetohydrodynamics (MHD), in which the dynamics of an ion-electron plasma is effectively captured by the center of mass fluid. In the limit of infinite conductivity, the magnetic field lines are frozen to the MHD fluid. However, for length scales comparable or inferior to  $d_i$  but superior to the electron inertial scale ( $d_e$ ), the ion and electron fluids are no longer coupled and the magnetic field lines are frozen only in the electron fluid. At those scales, one has to consider Hall

† Email address for correspondence: sbanerjee@iitk.ac.in

MHD (HMHD) model where the induction equation is given by

$$\partial_t \mathbf{b} - \eta \nabla^2 \mathbf{b} = \nabla \times (\mathbf{u} \times \mathbf{b}) - d_i \nabla \times (\mathbf{j} \times \mathbf{b}), \quad (1.1)$$

where  $\mathbf{u}$  is the velocity of the centre-of-mass fluid,  $\mathbf{b}$  is the magnetic field normalised to a velocity,  $\mathbf{j} = \nabla \times \mathbf{b}$  represents the current and the last term on the *r.h.s.* represents the Hall term. Similar to MHD, the total energy ( $\int (u^2 + b^2) / 2 d\tau$ ) is an inviscid invariant of HMHD. In fully developed HMHD turbulence, one therefore expects a universal energy cascade with constant flux rate  $\varepsilon$  across the extended inertial range comprising both MHD and Hall dominated sub-ion scales. In the realm of space and astrophysical plasmas, the cascade rate  $\varepsilon$  is pivotal to unravel the mechanisms behind magnetic reconnection, turbulent heating, small scale turbulent dynamos *etc.* (Huba & Rudakov 2004; Drake *et al.* 2008; Sahraoui *et al.* 2009; Bandyopadhyay *et al.* 2020; Andrés *et al.* 2019; Mininni *et al.* 2003, 2007). The analytical expressions of  $\varepsilon$ , obtained from exact relations in terms of two-point correlators or increments of relevant flow variables such as the velocity, the magnetic field *etc.* (Politano & Pouquet 1998; Galtier 2008; Banerjee & Galtier 2016; Andrés *et al.* 2018; Banerjee & Kritsuk 2018), are indeed used to calculate the turbulent heating rate using both numerical and observational data of plasma turbulence (Hellinger *et al.* 2018; Ferrand *et al.* 2019; Andrés *et al.* 2019). Interestingly, in Fourier space, the energy transfer induced by the Hall term is found to differ significantly from that of ordinary MHD. At MHD scales, the magnetic energy spectra follow a Kolmogorov-like  $k^{-5/3}$  power law whereas a  $k^{-7/3}$  spectrum emerges beyond the ion inertial scale (Krishan & Mahajan 2004*b,a*; Miura *et al.* 2019). In addition, for  $k < k_H$  ( $\sim d_i^{-1}$ ), the modal transfer rate of magnetic energy due to the Hall term becomes negative, leading to a back-scatter of magnetic energy to the large scales (Mininni *et al.* 2007; Gómez *et al.* 2010). To investigate the distinct nature of the energy transfers between MHD and Hall MHD in depth, it is customary to analyze in terms of the resonating energy conserving triads  $(\mathbf{k}, \mathbf{p}, \mathbf{q})$  such that  $\mathbf{k} + \mathbf{p} + \mathbf{q} = \mathbf{0}$ . The triads are said to be local if  $k \simeq p \simeq q$  whereas for nonlocal triads we have one of the sides to be significantly smaller or larger than the other two sides. On the other hand, the energy transfer is said to be local when the giver and the receiver modes are closely situated while the mediator mode, in principle, may be located anywhere. A local triad therefore always leads to local transfer whereas a nonlocal triad may associate a local or nonlocal transfer according as whether the giver and the receiver modes are of comparable sizes or not, respectively. Apart from small nonlocal transfers due to the energy containing large-scale structures in MHD (Cho 2010; Alexakis *et al.* 2005; Carati *et al.* 2006), the inertial scale energy transfers in both HD and MHD turbulence are predominantly mediated by the local triads (Kraichnan 1971; Verma *et al.* 2005). For HMHD turbulence, the situation becomes trickier. Whereas the total energy transfer remains local in nature, the energy transfer due to the Hall term shows clear signatures of nonlocality in the modal transfer of magnetic energy (Mininni *et al.* 2007; Gómez *et al.* 2010; Araki & Miura 2011). However, a dedicated study to investigate the possible source of such nonlocality is still awaited. Also in those studies, the energy transfer was simply interpreted as an exchange between different modes of the  $\mathbf{b}$ -fields only. However,  $\mathbf{j}$  and  $\mathbf{b}$  are functionally independent and can thus be considered as separate fields in mode-to-mode energy transfers. To be more specific, one can decompose the Hall term into two parts as  $\nabla \times (\mathbf{j} \times \mathbf{b}) = (\mathbf{b} \cdot \nabla) \mathbf{j} - (\mathbf{j} \cdot \nabla) \mathbf{b}$  and the corresponding energy transfer for each part can be studied individually. In analogy with ordinary MHD, the first part can be recognized as a  $\mathbf{j}$ -to- $\mathbf{b}$  transfer whereas the second part can be associated to a Hall induced  $\mathbf{b}$ -to- $\mathbf{b}$  transfer in spectral space. This decomposition is particularly interesting as the nature of triadic conservation for the two individual parts are structurally different as shown recently (Banerjee & Halder 2024).

The transfers through **b-to-b** channel are made up of three fundamental transfer units whereas transfers of **j-to-b** channel consist of five fundamental units. In addition, the contributions of these two channels have also been explored in the context of small-scale HMHD dynamo (Halder *et al.* 2023) where the **j-to-b** channel is found to be the primary contributors to the small scale turbulent Hall dynamo.

In this paper, using direct numerical simulations (DNS) of HMHD turbulence with  $512^3$  grid points, we thoroughly examine the locality (or nonlocality) of magnetic energy transfer through the aforesaid two channels. Employing shell-to-shell (S2S hereinafter) transfer rates, we calculate the local and nonlocal contributions for each part and identify the direction (direct or inverse) of the cascade. While both the channels contain signature of back transfer to large-scales, their scale-wise behaviour are found to differ significantly from each other. In particular, for the **j-to-b** channel, a change of nature of the local transfer is observed across the Hall wavenumber  $k_H$ . To further characterize the locality of the triads, we compute S2S transfer rates for a fixed giver shell (denoted as the mediator-specific transfer later) and find a prominent disparity between the two channels. Finally, assuming a heuristic power-law behaviour of the modal fields, we propose some quantitative comparison on the basis of our observed results.

The paper is organized as follows: in Sec. 2, we present the governing equations, the definition of the energy transfer rates and discuss the numerical methods along with the simulation details. Sec. 3 consists of calculation of S2S transfer rates with and without fixing the giver shell and a heuristic quantitative interpretation of our findings. Finally, in Sec. 4, we summarize and conclude.

## 2. Methodology

### 2.1. Governing equations and energy transfer rates

The inviscid incompressible HMHD equations are given by

$$\partial_t \mathbf{u} = -(\mathbf{u} \cdot \nabla) \mathbf{u} + (\mathbf{b} \cdot \nabla) \mathbf{b} - \nabla P_T, \quad (2.1)$$

$$\partial_t \mathbf{b} = -(\mathbf{u} \cdot \nabla) \mathbf{b} + (\mathbf{b} \cdot \nabla) \mathbf{u} + d_i (\mathbf{j} \cdot \nabla) \mathbf{b} - d_i (\mathbf{b} \cdot \nabla) \mathbf{j}, \quad (2.2)$$

$$\nabla \cdot \mathbf{u} = 0, \quad \nabla \cdot \mathbf{b} = 0, \quad (2.3)$$

where  $P_T = p + b^2/2$  is the total pressure. To examine the locality of the energy conserving triads, it is customary to obtain the evolution equations for  $n$ -th shell energy densities  $E_n^u$  and  $E_n^b$  as

$$\partial_t E_n^u = T_{n,m}^{u,u} + T_{n,m}^{u,b}, \quad (2.4)$$

$$\partial_t E_n^b = T_{n,m}^{b,b} + T_{n,m}^{b,u} + \mathcal{H}_{n,m}^{b,b} + \mathcal{H}_{n,m}^{b,j}, \quad (2.5)$$

where  $E_n^u = \sum_{|\mathbf{k}| \in n} \mathbf{u}_{\mathbf{k}} \cdot \mathbf{u}_{\mathbf{k}}^*/2$  and  $E_n^b = \sum_{|\mathbf{k}| \in n} \mathbf{b}_{\mathbf{k}} \cdot \mathbf{b}_{\mathbf{k}}^*/2$ , with  $\mathbf{u}_{\mathbf{k}}$  and  $\mathbf{b}_{\mathbf{k}}$  respectively denoting the Fourier transforms of  $\mathbf{u}(\mathbf{x})$  and  $\mathbf{b}(\mathbf{x})$  and  $T_{n,m}^{x,y}$  is the net transfer rate from the field  $y$  in shell  $m$  to the field  $x$  in shell  $n$  and is mathematically expressed as

$$|T_{n,m}^{x,y}| = \sum_{|\mathbf{k}| \in n} \sum_{|\mathbf{p}| \in m} \Im [(p \cdot z_q) (\mathbf{y}_{\mathbf{p}} \cdot \mathbf{x}_{\mathbf{k}})] \quad (2.6)$$

where  $\mathbf{x}$ ,  $\mathbf{y}$  and  $\mathbf{z}$  can be  $\mathbf{u}$  and  $\mathbf{b}$  with  $\Im$  denoting the imaginary part of a complex number. The algebraic sign becomes positive if  $\mathbf{x}$  and  $\mathbf{y}$  represent the same field. Similarly,  $\mathcal{H}_{n,m}^{b,b}$  and  $\mathcal{H}_{n,m}^{b,j}$  represent the transfer rates associated with  $d_i (\mathbf{j} \cdot \nabla) \mathbf{b}$  and  $-d_i (\mathbf{b} \cdot \nabla) \mathbf{j}$ ,

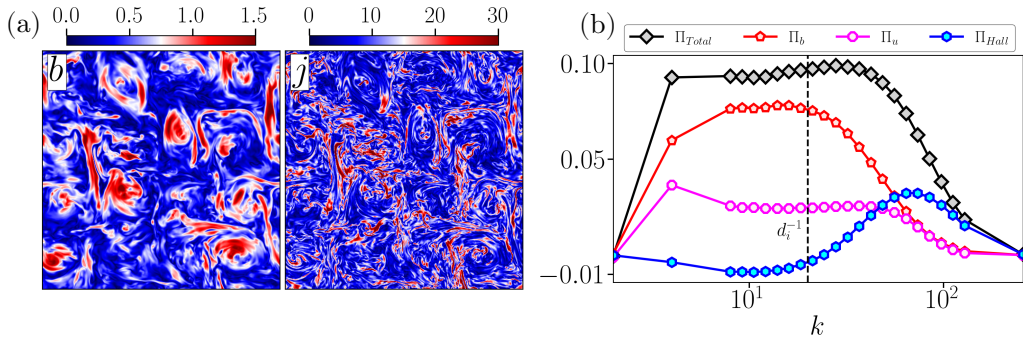


FIGURE 1. (a) Instantaneous slice of absolute values of magnetic (left) and current (right) fields at statistical steady state. Both fields show signature of a fully developed turbulent flow. (b) Various components of the total flux as function of wavenumber  $k$ . Here,  $\Pi_b$ ,  $\Pi_u$  and  $\Pi_{Hall}$  respectively denote flux rates for magnetic, kinetic energies and due to the Hall term with  $\Pi_{Total} = \Pi_b + \Pi_u + \Pi_{Hall}$ .

respectively and are written as

$$\mathcal{H}_{n,m}^{b,b} = -d_i \sum_{|\mathbf{k}| \in n} \sum_{|\mathbf{p}| \in m} \Im [(\mathbf{p} \cdot \mathbf{j}_q) (\mathbf{b}_p \cdot \mathbf{b}_k)], \quad (2.7)$$

$$\mathcal{H}_{n,m}^{b,j} = d_i \sum_{|\mathbf{k}| \in n} \sum_{|\mathbf{p}| \in m} \Im [(\mathbf{p} \cdot \mathbf{b}_q) (\mathbf{j}_p \cdot \mathbf{b}_k)]. \quad (2.8)$$

In the shell picture, the transfer is said to be local if the shell number  $n$  mostly receives energy from the neighboring shells whereas for the nonlocal transfers a non-negligible contribution also comes from the distant shells.

## 2.2. Numerical details

We solve (2.1) and (2.2) using a parallel pseudo-spectral code in a 3D periodic domain with  $512^3$  grid points. The box length is taken to be  $2\pi$  in each spatial direction. In our simulation, we take  $d_i = 0.05$  beyond which the Hall effect is expected to be visible. The aliasing error is removed with a standard 2/3-dealiasing method which fixes the maximum available wavenumber  $k_{max} \approx 170$  (Orszag 1971). A fourth-order Runge-Kutta (RK4) scheme is used for time integration and the time step is adjusted with CFL condition. The turbulence is generated and sustained by Taylor-Green (TG) forcing  $\mathbf{f} = f_0 [\sin(k_0 x) \cos(k_0 y) \cos(k_0 z), -\cos(k_0 x) \sin(k_0 y) \cos(k_0 z)]$  with  $f_0 = 0.5$  and  $k_0 = 2$ . A clear inertial range can be obtained if the dissipative terms contain higher order derivatives as compared to the nonlinear terms. In order to avoid the contamination of Hall contribution due to the usual dissipative effects ( $\sim \nabla^2$ ), here we employ a  $\nabla^4$ -hyperdiffusive operator in both the momentum and induction equation. Note that, the magnetic Prandtl number for our simulation is taken to be unity. All the numerical calculations are performed when the system reaches a statistical steady state balancing the average injection and dissipation of total energy. An instantaneous slice of the magnetic and current fields (see Fig. 1 (a)) shows the clear signature of fully-developed homogeneous turbulence. To capture a clear picture of the energy transfer in the inertial range, we construct 25 concentric shells with the radii:  $k_n \in \{0, 2, 4, 8, \dots, 128, 256\}$  where the radii between 8 and 128 is logarithmically binned with the ratio  $k_n/k_{n-1} = 1.14$ , between the subsequent shells. Note that, in our case, the inner and outer radii of the  $n$ -th shell are  $k_{n-1}$  and  $k_n$ , respectively. Using the aforementioned radii, we also calculate

the corresponding flux rates for kinetic energy, magnetic energy (MHD part) and the Hall term as

$$\Pi_u(k_0) = \sum_{|\mathbf{p}| \leq k_0} \sum_{|\mathbf{k}| > k_0} \Im [(\mathbf{p} \cdot \mathbf{u}_q)(\mathbf{u}_p \cdot \mathbf{u}_k) - (\mathbf{p} \cdot \mathbf{b}_q)(\mathbf{b}_p \cdot \mathbf{u}_k)], \quad (2.9)$$

$$\Pi_b(k_0) = \sum_{|\mathbf{p}| \leq k_0} \sum_{|\mathbf{k}| > k_0} \Im [(\mathbf{p} \cdot \mathbf{u}_q)(\mathbf{b}_p \cdot \mathbf{b}_k) - (\mathbf{p} \cdot \mathbf{b}_q)(\mathbf{u}_p \cdot \mathbf{b}_k)], \quad (2.10)$$

$$\Pi_{Hall}(k_0) = d_i \sum_{|\mathbf{p}| \leq k_0} \sum_{|\mathbf{k}| > k_0} \Im [(\mathbf{p} \cdot \mathbf{b}_q)(\mathbf{j}_p \cdot \mathbf{b}_k) - (\mathbf{p} \cdot \mathbf{j}_q)(\mathbf{b}_p \cdot \mathbf{b}_k)], \quad (2.11)$$

respectively.

### 3. Results and Discussion

#### 3.1. Calculation of shell-to-shell transfer rates

For length scales greater than  $d_i$  i.e.  $kd_i < 1$ , the magnetic energy transfer rate  $\Pi_b$  dominates over  $\Pi_u$  and  $\Pi_{Hall}$  (see Fig. 1 (b)). Similar to previous studies (Mininni *et al.* 2007; Gómez *et al.* 2010; Halder *et al.* 2023),  $\Pi_{Hall}$  becomes slightly negative across the said range of scales. However, for  $kd_i > 1$ ,  $\Pi_{Hall}$  becomes positive and takes over and exceeds  $\Pi_b$  and  $\Pi_u$  at sufficiently small scales. As a result, for  $kd_i < 1$ , the net magnetic energy transfer rate (MHD + Hall) decreases towards the small-scale whereas for  $kd_i > 1$ , it becomes amplified. All the above flux rates only provide the net transfer rate to a particular mode from all the others. In order to get a more detailed picture of the energy cascade and to investigate its localness, it is appropriate to study the corresponding S2S transfer rates using Eq. (2.6).

First, we examine  $T_{n,m}^{u,u}$  and  $T_{n,m}^{u,b}$  which denote the S2S transfer rates of kinetic energy through the  $\mathbf{u}$ -to- $\mathbf{u}$  and  $\mathbf{b}$ -to- $\mathbf{u}$  channels, respectively. For a given value of the receiver shell number  $n$ , if  $T_{n,m}^{x,y}$  is positive for  $n > m$  or negative for  $n < m$ , then we have a direct cascade and vice versa. From Fig. 2, both  $T_{n,m}^{u,u}$  and  $T_{n,m}^{u,b}$  represent a direct cascade which is mainly local in nature *i.e.* for a receiver shell number  $n$ , significant contribution only comes from the neighboring shells. In contrast, for both cases of cross-transfer  $T_{n,m}^{u,b}$  and  $T_{n,m}^{b,u}$ , a non-negligible nonlocal transfer is observed involving the scale of energy injection. This agrees with the previous findings of nonlocal transfers in MHD due to the effect of large-scale energy-containing structures (Alexakis *et al.* 2005; Cho 2010; Carati *et al.* 2006).

In Figs. 3 (a) and (b), we plot the S2S transfer rates corresponding to  $\mathbf{b}$ -to- $\mathbf{b}$  and  $\mathbf{j}$ -to- $\mathbf{b}$  channels of the Hall term as a function of giver and receiver shell numbers ( $m, n$ ), respectively. As it is apparent, both the channels are comprised of local and nonlocal transfers. For  $\mathcal{H}_{n,m}^{b,b}$ , close to the diagonal, for a fixed giver shell  $m$ , positive transfer is observed for a receiver shell  $n < m$  (red squares above the diagonal) whereas negative transfer is observed for a receiver shell  $n > m$  (blue squares below the diagonal). This clearly signifies an inverse transfer of magnetic energy due to the local interactions. On the other hand, far from the diagonal, the nature of the transfer is reversed and therefore a negative transfer is found above the diagonal while a positive transfer is found below the diagonal, indicating a direct nonlocal transfer of magnetic energy. Interestingly, the strength of the nonlocal transfers becomes gradually important at small-scales *i.e.* for large values of  $m$  and  $n$  (see Fig. 3 (a)). The nature of the energy transfer due to  $\mathcal{H}_{n,m}^{b,j}$ , on the other hand, is remarkably different (see Fig. 3 (b)). For shells with  $m, n < 12$ , both

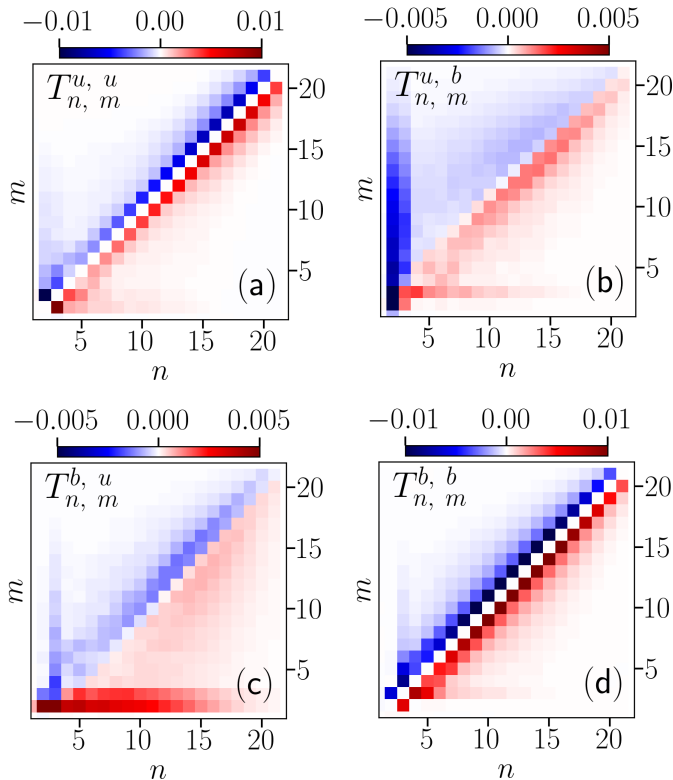


FIGURE 2. S2S transfer rates corresponding to MHD nonlinear terms as a function of giver and receiver shells ( $m, n$ ).  $T_{n,m}^{u,u}$  and  $T_{n,m}^{u,b}$  denote the transfer rate of kinetic energy through  $\mathbf{u}$ -to- $\mathbf{u}$ ,  $\mathbf{b}$ -to- $\mathbf{u}$  channels respectively.  $T_{n,m}^{b,u}$  and  $T_{n,m}^{b,b}$  denote the transfers rates of magnetic energy through  $\mathbf{u}$ -to- $\mathbf{b}$  and  $\mathbf{b}$ -to- $\mathbf{b}$  channels respectively.

the local and nonlocal transfer rates of  $\mathcal{H}_{n,m}^{b,j}$  are found to be relatively weaker compared to those of  $\mathcal{H}_{n,m}^{b,b}$  whereas the transfer rate considerably enhances at smaller scales where it is principally nourished by the local interactions. Furthermore, the color code of the transfers clearly indicates an inverse transfer of energy for small wavenumbers whereas the transfer becomes direct at sufficiently small scales. Interestingly, in both channels, a considerable transfer associating  $m, n = 3$  is observed which is possibly induced by the interaction between the injection scale and the Hall scale.

To further compare the strength of local and nonlocal transfer rates for the two channels of the Hall term, we plot  $\mathcal{H}_{n,m}^{b,b}$  and  $\mathcal{H}_{n,m}^{b,j}$  as function of  $m$  for  $n = 5, 9, 11, 13, 15$  and  $19$ , respectively (see Figs. 3 (c) and (d)). Such a diagram is useful to recognize the principal contributors for a fixed receiver shell  $n$ . For every single  $n$ , the peaks of the transfer are situated at neighboring shells indicating a predominant local transfer for  $\mathcal{H}_{n,m}^{b,b}$ . In addition, the amplitudes of the local transfers increase with receiver shell number  $n$  running from 5 to 15. A similar trend is also observed for the negative transfers at large  $m$ . These two features offer an alternative way to delineate the increasing strength of both the local and nonlocal transfers at small-scales. For  $n = 19$ , however, the amplitude for the local transfer is found to decrease along with a substantial nonlocal contribution from small values of  $m$ . For  $\mathcal{H}_{n,m}^{b,j}$ , the situation is notably different. For  $n < 15$ , we observe a comparatively weaker inverse transfer made up of commensurate contributions both

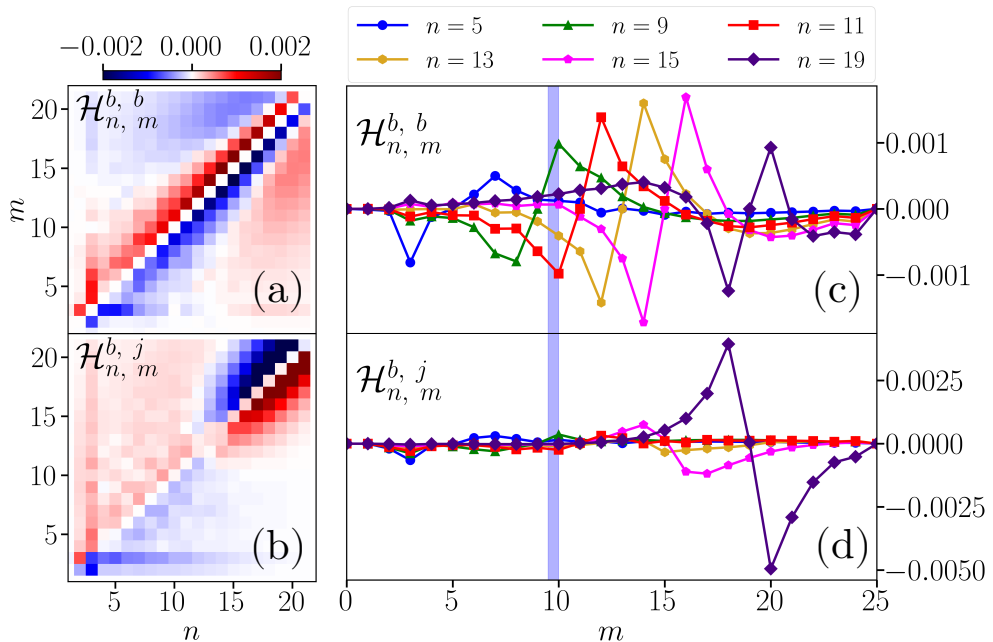


FIGURE 3. (a) and (c) S2S transfer rate for **b-to-b** channel of the Hall term as a function of giver and receiver shell numbers ( $m, n$ ). (b) and (d) Same for **j-to-b** channel as a function of giver and receiver shell numbers ( $m, n$ ).

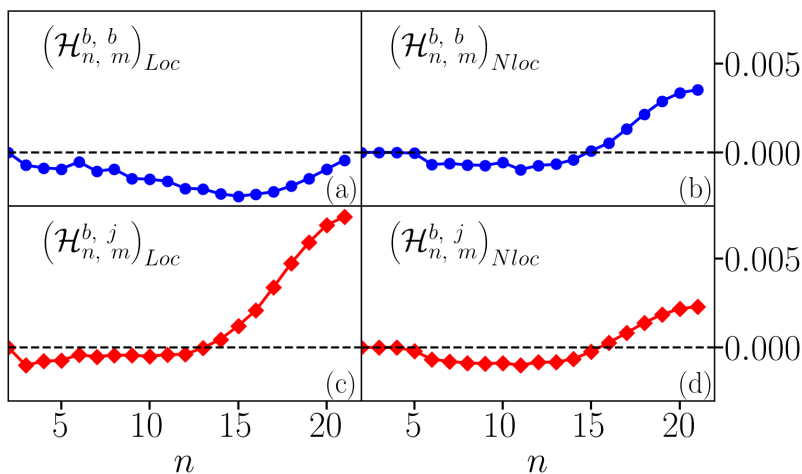


FIGURE 4. (a) and (b) Local and nonlocal magnetic energy transfer rates due to  $\mathcal{H}_{n,m}^{b,b}$  as a function of  $n$ , respectively. (c) and (d) Similar plots for  $\mathcal{H}_{n,m}^{b,j}$ . For a given  $n$ , the local transfers rates are computed only for  $m = n - 1$  and  $n - 2$ .

from local and nonlocal giver shells. For  $n = 15$  and beyond, the direction of the energy transfer flips and local contributions become quite large with respect to the nonlocal contributions. Interestingly, similar to the  $\mathcal{H}_{n,m}^{b,b}$ , here also a considerable (both local and nonlocal) transfer is observed around  $m, n = 3$ .

In order to exclusively capture the contributions from the local shells, we calculate the total magnetic energy flux rate up to second nearest neighbour shell (see Figs. 4

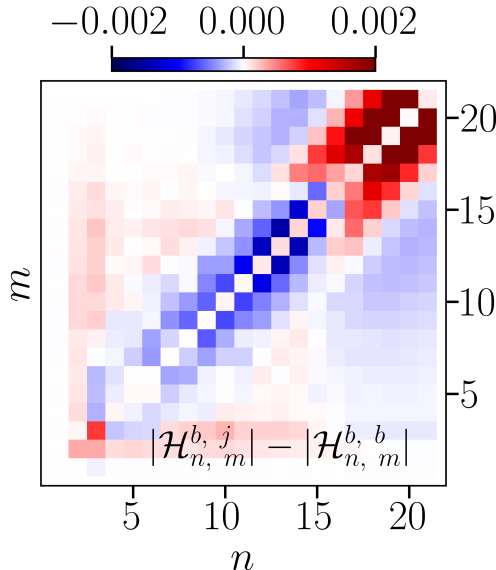


FIGURE 5.  $|\mathcal{H}_{n,m}^{b,j}| - |\mathcal{H}_{n,m}^{b,b}|$  as a function of giver-receiver shell numbers  $(m,n)$ .

(a) and (c)). As an example, for receiver shell  $n$ , the total flux rate is computed for giver shells  $m = n - 1$  and  $m = n - 2$ . As expected, for lower wavenumbers, the local contribution for **b-to-b** channel is stronger compared to **j-to-b** channel. Around shell number 15, the local contribution of the latter sharply increases and becomes positive signifying direct S2S transfer. Evidently, the local contributions for the **j-to-b** channel is primarily responsible for the observed enhancement of magnetic energy transfer towards smaller scales discussed previously. In contrast, the nonlocal contributions for both **b-to-b** and **j-to-b** channels are inverse and of comparable magnitudes for shells below  $n = 15$ . Beyond that, both become direct with  $\mathcal{H}_{n,m}^{b,b}$  being slightly greater than  $\mathcal{H}_{n,m}^{b,j}$  (see Figs. 4 (b) and (d)).

Finally, to summarize the relative strength of the two channels of the Hall term, in Fig. 5, we plot  $|\mathcal{H}_{n,m}^{b,j}| - |\mathcal{H}_{n,m}^{b,b}|$  as a function of  $(m,n)$ . For a given  $(m,n)$ , positive and negative values of the transfer rate respectively denote the dominance of  $|\mathcal{H}_{n,m}^{b,j}|$  and  $|\mathcal{H}_{n,m}^{b,b}|$ , respectively. As it is apparent, local transfers in smaller scales (high values of  $m$  and  $n$ ) are dominated by  $\mathcal{H}_{n,m}^{b,j}$  whereas large-scale (low values of  $m$  and  $n$ ) local transfers are primarily governed by  $\mathcal{H}_{n,m}^{b,b}$ . For the nonlocal transfers, on the other hand, the regions with  $m > n$  is dominated by  $\mathcal{H}_{n,m}^{b,j}$  whereas  $\mathcal{H}_{n,m}^{b,b}$  becomes important for  $m < n$ .

### 3.2. Calculation of mediator specific S2S transfers

The S2S transfer rates, discussed so far, examine the locality of transfer between a pair of giver-receiver shells  $(m,n)$  without any information regarding the location of the mediator mode  $(q)$ . However, the knowledge of  $q$  is essential to distinguish between local transfers (comparable giver and receiver wavenumbers) mediated by local ( $k \simeq p \simeq q$ ) and elongated triads ( $k \simeq \gg q$ ). For HD and MHD, local transfer via nonlocal triads are found to play important role in the inertial energy cascade (Mininni *et al.* 2006, 2008; Alexakis *et al.* 2005; Cho 2010). In order to investigate the same due to the Hall term,

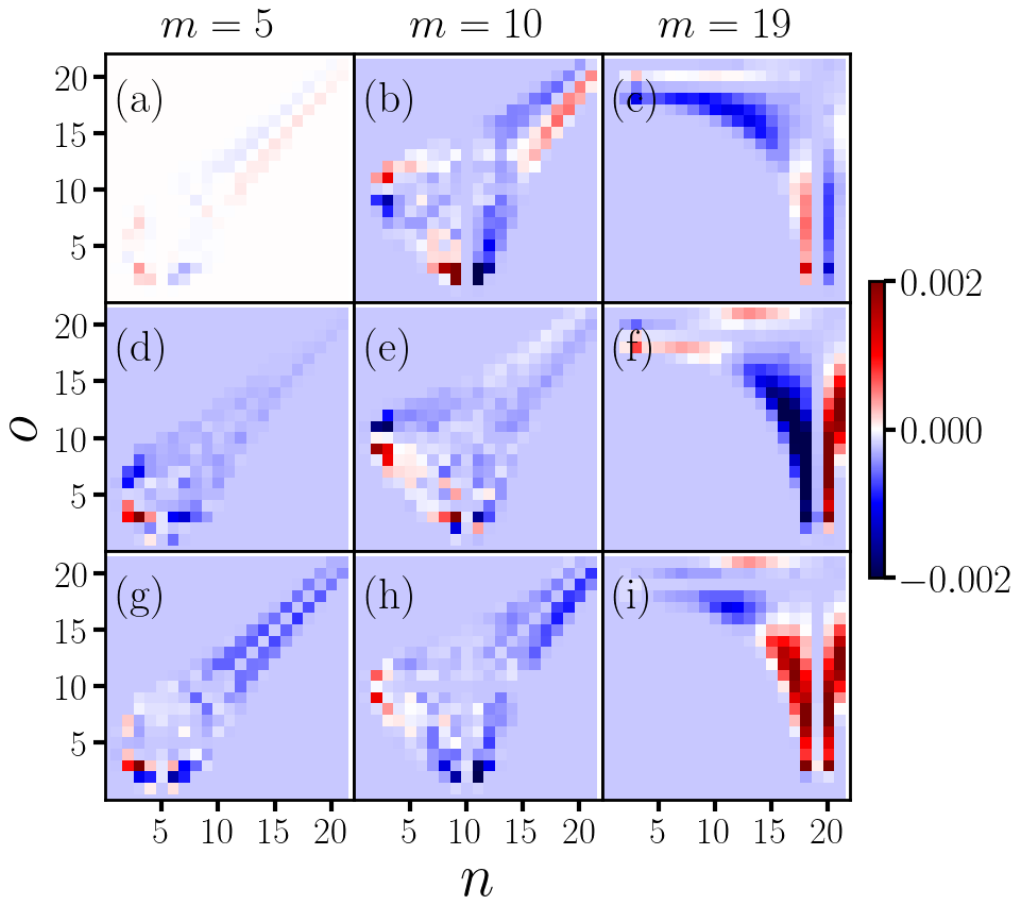


FIGURE 6. Top row:  $\mathcal{H}_{n,m,o}^{b,b}$  as a function of mediator and receiver shell numbers  $(o,n)$  for a giver shell number  $m$ . Middle row:  $\mathcal{H}_{n,m,o}^{b,j}$  as a function of mediator and receiver shell numbers  $(o,n)$  for a giver shell number  $m$ . Bottom row:  $|\mathcal{H}_{n,m,o}^{b,j} - \mathcal{H}_{n,m,o}^{b,b}|$ .

we calculate the energy transfer rates as a function of  $m,n$  and mediator shell  $o$ :

$$\mathcal{H}_{n,m,o}^{b,b} = -d_i \sum_{|\mathbf{k}| \in n} \sum_{|\mathbf{q}| \in o} \sum_{|\mathbf{p}| \in m} \Im [(\mathbf{p} \cdot \mathbf{j}_q) (\mathbf{b}_p \cdot \mathbf{b}_k)], \quad (3.1)$$

$$\mathcal{H}_{n,m,o}^{b,j} = d_i \sum_{|\mathbf{k}| \in n} \sum_{|\mathbf{q}| \in o} \sum_{|\mathbf{p}| \in m} \Im [(\mathbf{p} \cdot \mathbf{b}_q) (\mathbf{j}_p \cdot \mathbf{b}_k)]. \quad (3.2)$$

In top and middle rows of Fig. 6, we plot  $\mathcal{H}_{n,m,o}^{b,b}$  and  $\mathcal{H}_{n,m,o}^{b,j}$  for  $m = 5, 10$  and  $19$ , respectively. Due to the logarithmic binning in the inertial range, these choices of giver shells approximately corresponds to wavenumbers  $\approx 10, 20, 70$  which captures three regions of  $kd_i < 1$ ,  $kd_i \sim 1$  and  $kd_i > 1$ , respectively. For  $\mathcal{H}_{n,m,o}^{b,b}$ , regions with weak local transfer is observed for  $m = 5$  and close to  $o = 5$ , corresponding to local triads where  $k \simeq p \simeq q$  (see bottom left of Fig. 6 (a)). Note that, for a fixed  $m,n$ , we define the triads to be local if  $|o - m| \leq 2$  or  $|o - n| \leq 2$  and nonlocal otherwise. Another region with a weak but non-zero nonlocal transfer can be identified for  $n, o \gg m$  which naturally associate highly nonlocal triads with  $k \simeq q \gg p$  (from center to top right of Fig. 6 (a)). For  $m = 10$ , the most intense region of local transfer occurs for  $o = 2$  and

3 associating nonlocal triads with  $k \simeq p \gg q$  (deep red and blue squares at the bottom of Fig. 6 (b)). In this case, two regions of substantial nonlocal transfers are also evident: (i)  $m \simeq o \gg n$  corresponding to triads  $p \simeq q \gg k$  (blue and red squares at the center left) and (ii)  $n \simeq o \gg m$  corresponding to triads  $k \simeq q \gg p$  (elongated region at top right). Finally, for  $m = 19$ , a similar region of moderate local transfers through nonlocal triads  $k \simeq p \gg q$  is observed up to  $o \approx 12$  (moderate blue and red squares at bottom right of Fig. 6 (c)). Beyond this, a horizontal spread towards smaller  $n$  values emerges, indicating nonlocal energy transfer involving nonlocal triads where  $p \simeq q \gg k$ .

For  $m = 5$ , unlike the previous case, local transfers of  $\mathcal{H}_{n, m, o}^{b, j}$  with local triads become significant close to  $o = 5$ . As with  $\mathcal{H}_{n, m, o}^{b, b}$ , the nonlocal transfer for  $n \simeq o \gg m$  remains extremely weak for this channel (see Fig. 6 (d)). For  $m = 10$ , similar regions of non-negligible local transfer via nonlocal triads  $k \simeq p \gg q$  and nonlocal transfer with nonlocal triads  $p \simeq q \gg k$  (dark red and blue squares in the center left of Fig. 6 (e)) are also observed. However, in contrast to  $\mathcal{H}_{n, m, o}^{b, b}$ , no substantial nonlocal transfer is evident for the  $k \simeq q \gg p$  triads (elongated top right section). For  $m = 19$ , a region of strong local transfer mediated by nonlocal triads persists up to  $o \approx 12$ . Beyond which a horizontal spread of diminishing intensity towards smaller  $n$  values is observed, suggesting nonlocal energy transfer through triads with  $p \simeq q \gg k$  (see Fig. 6 (f)).

Finally, to compare relative strengths of  $\mathcal{H}_{n, m, o}^{b, b}$  and  $\mathcal{H}_{n, m, o}^{b, j}$ , we compute the difference  $|\mathcal{H}_{n, m, o}^{b, j}| - |\mathcal{H}_{n, m, o}^{b, b}|$  for  $m = 5, 10$  and  $19$  (Fig. 6 bottom row). For each  $(o, n)$  pair, positive values indicate the dominance of  $|\mathcal{H}_{n, m, o}^{b, j}|$  whereas negative values indicate dominance of  $|\mathcal{H}_{n, m, o}^{b, b}|$ . As it evident, for  $m = 5$ , the strength of the local transfers with local triads are comparable for the two channels despite a slight dominance of  $|\mathcal{H}_{n, m, o}^{b, b}|$  in the region governed by nonlocal transfers (elongated top right section of Fig. 6 (g)). For  $m = 10$ ,  $|\mathcal{H}_{n, m, o}^{b, b}|$  is stronger for regions of local transfer via nonlocal triads (bottom middle of Fig. 6 (h)) as well as in the nonlocal transfer regime via nonlocal triads  $k \simeq q \gg p$  (see elongated top right section). However,  $|\mathcal{H}_{n, m, o}^{b, j}|$  takes over in the nonlocal transfer regime associating  $p \simeq q \gg k$  triads (see left middle section). Finally, for  $m = 19$ ,  $|\mathcal{H}_{n, m, o}^{b, j}|$  clearly dominate in the region of local transfer through nonlocal triads (dark red squares at bottom right of Fig. 6 (i)). However,  $|\mathcal{H}_{n, m, o}^{b, b}|$  slightly takes over  $|\mathcal{H}_{n, m, o}^{b, j}|$  in the nonlocal energy transfer regime involving triads with  $p \simeq q \gg k$  (see moderate blue squares at center top).

### 3.3. Quantitative estimation using heuristic power laws

In the preceding discussion, we have identified different types of triads that contribute to the local and nonlocal transfer of magnetic energy due to the Hall term. These are broadly classified into four categories: (i)  $k \simeq p \simeq q$ , (ii)  $k \simeq p \gg q$ , (iii)  $k \simeq q \gg p$  and (iv)  $p \simeq q \gg k$  (see Fig. 7 (a)). Triads of type (i) and (ii) are primarily involved in local transfers whereas types (iii) and (iv) partake in nonlocal transfers. Now, we provide an estimation of the observed transfer rates for each type of triad following a framework motivated by [Aluie & Eyink \(2009, 2010\)](#). For a given triad  $(\mathbf{k}, \mathbf{p}, \mathbf{q})$ , we can define

$$\mathcal{R} = \frac{|\mathcal{H}_{n, m, o}^{b, b}|}{|\mathcal{H}_{n, m, o}^{b, j}|} \approx \frac{d_i p j_q b_p b_k}{d_i p b_q j_p b_k} = \frac{d_i j_q b_p}{d_i b_q j_p}, \quad (3.3)$$

where  $\mathcal{R}$  can be taken as a measure of relative strength of the two channels. To proceed further, the information regarding the dependence of  $b_k$  and  $j_k$  on  $k$  is required. Assuming a self-similar cascade for magnetic energy, one can write  $E_b(k) \sim b_k^2 \sim k^{-\alpha} \implies b_k \sim$

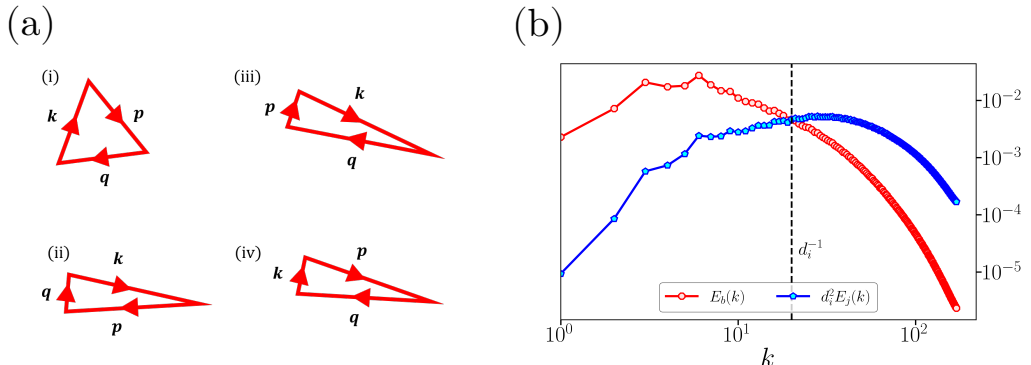


FIGURE 7. (a) Schematic diagram of contributing triads involved in local and nonlocal transfers and (b) spectra for magnetic energy (red) and squared current density multiplied by  $d_i^2$  (blue) as a function of wavenumber  $k$ . The dashed vertical line denotes the Hall scale  $\approx 1/d_i$ .

$k^{-\alpha/2}$  where  $\alpha = 5/3$  and  $7/3$  for  $kd_i < 1$  and  $kd_i > 1$ , respectively (see red curve in Fig. 7 (b)). Similarly, for the current field (multiplied by  $d_i$ ), one can write  $d_i j_k \sim k^{-\beta/2}$  where  $\beta = -1/3$  and  $1/3$  for  $kd_i < 1$  and  $kd_i > 1$ , respectively (see blue curve in Fig. 7 (b)). For the local triads of type (i), Eq. (3.3) yields  $\mathcal{R} \sim 1$  both for wavenumbers smaller and larger than the Hall wavenumber  $k_H$ . This indicates that contributions from  $\mathcal{H}_{n,m,o}^{b,b}$  and  $\mathcal{H}_{n,m,o}^{b,j}$  are of comparable strength, in agreement with patterns observed in Figs. 6 (a), (d) and (g). In contrast, local transfers via nonlocal triads of type (ii) result in  $\mathcal{R} \ll 1$ , irrespective of the position of the wavenumbers, indicating dominance of  $\mathcal{H}_{n,m,o}^{b,j}$  over  $\mathcal{H}_{n,m,o}^{b,b}$ . This is also evident from Figs. 6 (c), (f) and (i). Triads of type (iii) give  $\mathcal{R} \gg 1$  leading to comparatively stronger  $\mathcal{H}_{n,m,o}^{b,b}$ , consistent with observed enhanced values seen in the top right regions of all the sub-figures of Fig. 6 with  $m = 5$  and 10.

Despite some good agreements, interpretation of certain aspects of the observed results remain elusive. For instance, nonlocal triads of type (ii) yield  $\mathcal{R} \ll 1$  which does not align well with the observations in Figs. 6 (b), (e) and (h). Similarly, triads of type (iv) result in  $\mathcal{R} \sim 1$ , indicating comparable nonlocal contributions from the two channels. However, this is also not strongly supported by preceding discussion on Fig. 6. These apparent discrepancies may stem from the approximations inherent in Eq. (3.3) as well as the limited resolution of the current simulation. Improved agreement between numerical observations and theoretical results may be achievable through a more rigorous analytical framework combined with higher resolution simulations.

#### 4. Summary and conclusion

In this work, we have numerically explored the locality of energy transfer in three-dimensional HMHD turbulence. In particular, we focus on the local and non-local energy transfers due to the Hall term. By decomposing the Hall term into two parts, we elucidate the nature of nonlocal interactions in **b-to-b** and **j-to-b** channels individually. By computing S2S transfer rates between a pair of giver-receiver shells ( $m, n$ ), we find that **b-to-b** channel exhibits a strongly local inverse transfer of magnetic energy for all the wavenumbers. Additionally, this channel shows a nonlocal direct transfer that increases at large wavenumbers. On the other hand, both the local and nonlocal inverse transfers of **j-to-b** remain relatively weak up to shell number 15. Beyond that, the sign of the transfer

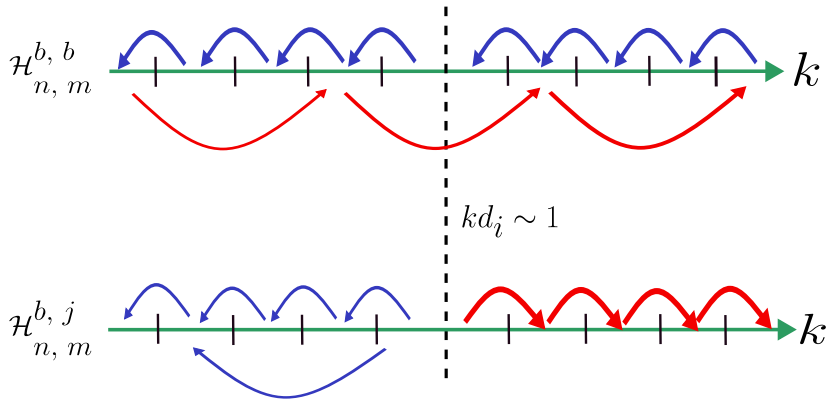


FIGURE 8. Schematic diagram summarizing the nature of cascade for the two channels of the Hall term. The thickness of the arrows are indicative of the intensity of the transfers.

reverses, becoming direct, accompanied by an increase in intensity of local transfers (see Figs. 3 and 4, also Fig. 8 for a schematic diagram).

To further examine the nature of fundamental triad interactions, we computed S2S transfer rates for a fixed receiver shell  $m$ . Both  $\mathcal{H}_{n,m,o}^{b,b}$  and  $\mathcal{H}_{n,m,o}^{b,j}$  display weak transfer rates corresponding to local transfers via local triads. However, strong local cascade for  $\mathbf{b}-\mathbf{b}$  channel at all wavenumbers and for  $\mathbf{j}-\mathbf{b}$  channels at higher wavenumbers indicate that the major contribution of local transfer arises from nonlocal triads of type  $k \simeq p \gg q$  (see Fig. 3). Nonlocal transfers involve two distinct triad configurations  $k \simeq q \gg p$  and  $p \simeq q \gg k$  (see types (iii) and (iv) in Fig. 7 (a)). Whereas  $\mathcal{H}_{n,m,o}^{b,b}$  is predominantly made up of the first kind of non-local triads, leading to enhanced nonlocal transfer at large wavenumbers, the second type of nonlocal triads are largely present in  $\mathcal{H}_{n,m,o}^{b,j}$  at moderate wavenumbers (Fig. 3).

The current work gives a detailed picture of fundamental triadic interactions responsible for nonlocality and backscatter of energy as reported in earlier studies (Mininni *et al.* 2007; Gómez *et al.* 2010). Our results demonstrate that nonlocal triads play a significant role both in the local and nonlocal transfers via  $\mathbf{b}-\mathbf{b}$  and  $\mathbf{j}-\mathbf{b}$  channels. The existing shell model, as the one proposed by Galtier & Buchlin (2007), is developed assuming local interactions through local triads only. Our findings mandate a revisit of the same to include additional triadic interactions. A detailed understanding of HMHD turbulence is also crucial in studying sub-ion scale turbulence in astrophysical plasmas such as solar wind and magnetospheric plasmas. With the advent of high resolution plasma measurements from multi-spacecraft missions like MMS, it is now possible to directly measure the heating rate associated with different channels of the Hall term. Our work further contributes to this effort by enabling a separate estimation of heating contributions from local and nonlocal interactions. The eddy-damped quasi normal Markovian (EDQNM) approximation has been shown to replicate observed locality of energy transfer both in HD and MHD turbulence. A similar investigation for HMHD turbulence to compare the observed results remains a subject for future study.

## Acknowledgments

A.H. and S.B. acknowledge the financial support from STC-ISRO grant (STC/PHY/20236640). The simulation code is developed by A.H. following the parallelization

schemes in [Mortensen & Langtangen \(2016\)](#). The simulation is performed using the support and resources provided by PARAM Sanganak under the National Supercomputing Mission, Government of India at the Indian Institute of Technology, Kanpur.

## Declaration of interests

The authors report no conflict of interest.

## REFERENCES

- ALEXAKIS, A., MININNI, P. D. & POUQUET, A. 2005 Imprint of large-scale flows on turbulence. *Phys. Rev. Lett.* **95**, 264503.
- ALEXAKIS, A., MININNI, P. D. & POUQUET, A. 2005 Shell-to-shell energy transfer in magnetohydrodynamics. I. Steady state turbulence. *Phys. Rev. E* **72** (4), 046301.
- ALUIE, H. & EYINK, G. L. 2009 Localness of energy cascade in hydrodynamic turbulence. ii. sharp spectral filter. *Physics of Fluids* **21** (11), 115108.
- ALUIE, H. & EYINK, G. L. 2010 Scale locality of magnetohydrodynamic turbulence. *Phys. Rev. Lett.* **104**, 081101.
- ANDRÉS, N., GALTIER, S. & SAHRAOUI, F. 2018 Exact law for homogeneous compressible hall magnetohydrodynamics turbulence. *Phys. Rev. E* **97**, 013204.
- ANDRÉS, NAHUEL, SAHRAOUI, FOUAD, GALTIER, SEBASTIEN, HADID, LINA Z, FERRAND, RENAUD & HUANG, SHIYONG Y 2019 Energy cascade rate measured in a collisionless space plasma with mms data and compressible hall magnetohydrodynamic turbulence theory. *Physical review letters* **123** (24), 245101.
- ARAKI, KEISUKE & MIURA, HIDEAKI 2011 Nonlocal interaction of inverse magnetic energy transfer in hall magnetohydrodynamic turbulence. *Plasma and Fusion Research* **6**, 2401132–2401132.
- BANDYOPADHYAY, RIDDIHI, SORRISO-VALVO, LUCA, CHASAPIS, ALEXANDROS, HELLINGER, PETR, MATTHAEUS, WILLIAM H, VERDINI, ANDREA, LANDI, SIMONE, FRANCI, LUCA, MATTEINI, LORENZO, GILES, BARBARA L & OTHERS 2020 In situ observation of hall magnetohydrodynamic cascade in space plasma. *Physical review letters* **124** (22), 225101.
- BANERJEE, SUPRATIK & GALTIER, SÉBASTIEN 2016 An alternative formulation for exact scaling relations in hydrodynamic and magnetohydrodynamic turbulence. *Journal of Physics A: Mathematical and Theoretical* **50** (1), 015501.
- BANERJEE, SUPRATIK & HALDER, ARIJIT 2024 Fundamental units of triadic interactions in Hall magnetohydrodynamic turbulence: How far can we go? *Physics of Plasmas* **31** (6), 062301.
- BANERJEE, SUPRATIK & KRITSUK, ALEXEI G 2018 Energy transfer in compressible magnetohydrodynamic turbulence for isothermal self-gravitating fluids. *Physical Review E* **97** (2), 023107.
- CARATI, D., DEBLIQUY, O., KNAEPEN, B., TEACA, B. & VERMA, M. 2006 Energy transfers in forced mhd turbulence. *J. Turbul.* **7**, 1–12.
- CHO, JUNGYEON 2010 Non-locality of hydrodynamic and magnetohydrodynamic turbulence. *The Astrophysical Journal* **725** (2), 1786.
- DRAKE, J. F., SHAY, M. A. & SWISDAK, M. 2008 The hall fields and fast magnetic reconnection. *Physics of Plasmas* **15** (4), 042306.
- FERRAND, R., GALTIER, S., SAHRAOUI, F., MEYRAND, R., ANDRÉS, N. & BANERJEE, S. 2019 On exact laws in incompressible hall magnetohydrodynamic turbulence. *The Astrophysical Journal* **881** (1), 50.
- GALTIER, SÉBASTIEN 2008 von kármán–howarth equations for hall magnetohydrodynamic flows. *Phys. Rev. E* **77**, 015302(R).
- GALTIER, SÉBASTIEN & BUCHLIN, ERIC 2007 Multiscale hall-magnetohydrodynamic turbulence in the solar wind. *The Astrophysical Journal* **656** (1), 560.
- GÓMEZ, DANIEL O, MININNI, PABLO D & DMITRUK, PABLO 2010 Hall-magnetohydrodynamic small-scale dynamos. *Physical Review E* **82** (3), 036406.

- HALDER, ARIJIT, BANERJEE, SUPRATIK, CHATTERJEE, ANANDO G. & SHARMA, MANOHAR K. 2023 Contribution of the hall term in small-scale magnetohydrodynamic dynamos. *Phys. Rev. Fluids* **8**, 053701.
- HELLINGER, PETR, VERDINI, ANDREA, LANDI, SIMONE, FRANCI, LUCA & MATTEINI, LORENZO 2018 von kármán–howarth equation for hall magnetohydrodynamics: hybrid simulations. *The Astrophysical Journal Letters* **857** (2), L19.
- HUBA, J. D. & RUDAKOV, L. I. 2004 Hall magnetic reconnection rate. *Phys. Rev. Lett.* **93**, 175003.
- KRAICHNAN, R. H. 1971 Inertial-range transfer in two- and three-dimensional turbulence. *Journal of Fluid Mechanics* **47** (3), 525–535.
- KRISHAN, V & MAHAJAN, SM 2004a Hall-mhd turbulence in the solar atmosphere. *Solar Physics* **220**, 29–41.
- KRISHAN, V. & MAHAJAN, S. M. 2004b Magnetic fluctuations and hall magnetohydrodynamic turbulence in the solar wind. *Journal of Geophysical Research: Space Physics* **109** (A11).
- MININNI, P. D., ALEXAKIS, A. & POUQUET, A. 2006 Large-scale flow effects, energy transfer, and self-similarity on turbulence. *Phys. Rev. E* **74**, 016303.
- MININNI, PABLO D, ALEXAKIS, ALEXANDROS & POUQUET, ANNICK 2007 Energy transfer in hall-mhd turbulence: cascades, backscatter, and dynamo action. *Journal of plasma physics* **73** (3), 377–401.
- MININNI, P. D., ALEXAKIS, A. & POUQUET, A. 2008 Nonlocal interactions in hydrodynamic turbulence at high reynolds numbers: The slow emergence of scaling laws. *Phys. Rev. E* **77**, 036306.
- MININNI, PABLO D., GOMEZ, DANIEL O. & MAHAJAN, SWADESH M. 2003 Dynamo action in magnetohydrodynamics and hall-magnetohydrodynamics. *The Astrophysical Journal* **587** (1), 472–481.
- MIURA, HIDEAKI, YANG, JIGUAN & GOTOH, TOSHIYUKI 2019 Hall magnetohydrodynamic turbulence with a magnetic prandtl number larger than unity. *Phys. Rev. E* **100**, 063207.
- MORTENSEN, MIKAEL & LANGTANGEN, HANS PETTER 2016 High performance python for direct numerical simulations of turbulent flows. *Computer Physics Communications* **203**, 53–65.
- ORSZAG, STEVEN A. 1971 On the elimination of aliasing in finite-difference schemes by filtering high-wavenumber components. *Journal of Atmospheric Sciences* **28** (6), 1074 – 1074.
- POLITANO, H. & POUQUET, A. 1998 von kármán–howarth equation for magnetohydrodynamics and its consequences on third-order longitudinal structure and correlation functions. *Phys. Rev. E* **57**, R21–R24.
- SAHRAOUI, F., GOLDSTEIN, M. L., ROBERT, P. & KHOTYAINTEV, YU. V. 2009 Evidence of a cascade and dissipation of solar-wind turbulence at the electron gyroscale. *Phys. Rev. Lett.* **102**, 231102.
- VERMA, MAHENDRA K., AYYER, ARVIND & CHANDRA, AMAR V. 2005 Energy transfers and locality in magnetohydrodynamic turbulence. *Physics of Plasmas* **12** (8), 082307.